Micromachined Waveguide Integrated RF MEMS Switch Operating between 500-750 GHz

U. SHAH[1], T. RECK[2], E. DECROSSAS[2], C. JUNG-KUBIAK[2], H. FRID[1], G. CHATTOPADHYAY[2], I. MEHDI[2], and J. OBERHAMMER[1]

[1]KTH Royal Institute of Technology, Stockholm, Sweden
[2]Jet Propulsion Laboratory, Pasadena, CA, 91109 USA

Abstract. This paper presents a 500-750 GHz waveguide based single-pole single-throw (SPST) switch achieving a 40% bandwidth. It is the first ever RF MEMS switch reported to be operating above 220 GHz. The switch is based on a MEMS-reconfigurable surface which can block the wave propagation in the waveguide by short-circuiting the electrical field lines of the TE10 mode. The switch is designed for optimized isolation in the blocking state and for optimized insertion loss in the non-blocking state. The measurement results of the first prototypes show better than 15 dB isolation in the blocking state and better than 3 dB insertion loss in the non-blocking state for 500-750 GHz. The higher insertion loss is mainly attributed to the insufficient metal thickness and surface roughness on the waveguide sidewalls. Two switch designs with different number of blocking elements are fabricated and compared. The overall switch bandwidth is limited by the waveguide only and not by the switch technology itself.

Index Terms. Micromachined waveguide, RF MEMS, waveguide switch, switch, submillimeter-wave, terahertz, THz.

1. Introduction

The submillimeter-wave frequency band has an increasing scientific and industrial interest because of its applications in spectroscopy, radar, imaging systems, radio astronomy, material characterization, and ultra-high bandwidth wireless data communication. The unavailability of commercial components at these frequencies [1] creates the terahertz gap which presents an opportunity for devices based on Microelectromechanical systems (MEMS). MEMS devices are ideal for submillimeter-wave applications because of their low loss, low power consumption, high linearity and large bandwidth. MEMS based waveguide switches can replace the conventional rotary motor-based mechanical switches

which are bulky, heavy, requires high power and have a very slow response time. MEMS waveguide switches using electrostatic actuators have already been implemented [2] and more recently the actuators have been integrated inside the waveguide channel [3]. Moreover, MEMS based waveguide switches have been shown to perform well up to a frequency of 110 GHz [4]. MEMS-based RF devices are rare above 110 GHz and so far only two devices: a switchable stub [5] and a phase shifter [6] have been reported by the authors functioning up to a maximum frequency of 600 GHz. In addition, micromachined waveguides have shown promising results even up to 2.7 THz [7].

In this paper, we report on a fully functional RF MEMS waveguide switch based on a MEMS-reconfigurable surface operating at the center frequency of 625 GHz and with a bandwidth of 40 % in the frequency band between 500-750 GHz. It is the first ever RF MEMS switch operating above 220 GHz. The bandwidth of the switch is limited only by the waveguide and not by the switch technology itself.

2. Concept and Design

The single-pole single-throw (SPST) switch concept is shown in Fig. 1 and it is based on a MEMS reconfigurable surface inserted perpendicular to the wave propagation. The MEMS reconfigurable surface can short-circuit the electrical field lines in the TE_{10} mode thus blocking the wave propagation. It consists of vertical columns forming the contact cantilevers which are connected to horizontal bars. The contact cantilevers are grouped into a set of fixed and a set of movable cantilevers. The fixed set is anchored and the movable set is mechanically connected to electrostatic comb drive MEMS actuators via the horizontal bars. The

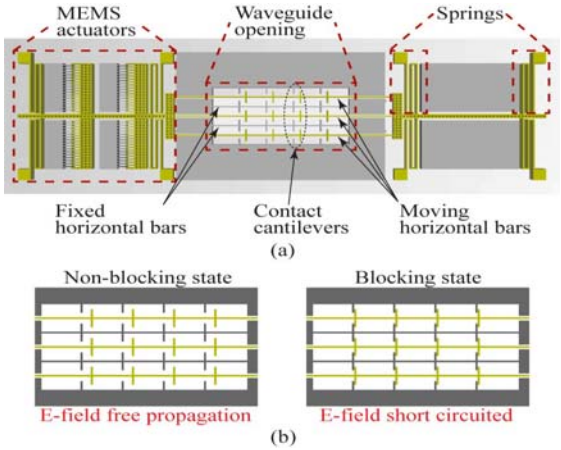

Fig.1. MEMS waveguide switch concept: (a) schematic cross-section of the switch, and (b) Non-blocking and blocking state of the switch.

comb-drives are placed to one side of narrow walls of the waveguide. In the non-blocking state (Fig. 1b), the vertical columns are not in contact and thus allow the electromagnetic wave to propagate freely through the MEMS reconfigurable surface. In the blocking state (Fig. 1b), the movable vertical columns are laterally displaced by the electrostatic actuators and brought into contact with the fixed vertical columns. This forms closed vertical columns in the path of the wave propagation, therefore blocking the electromagnetic wave propagation through the MEMS reconfigurable surface by short-circuiting the electric field lines of the dominant TE_{10} mode.

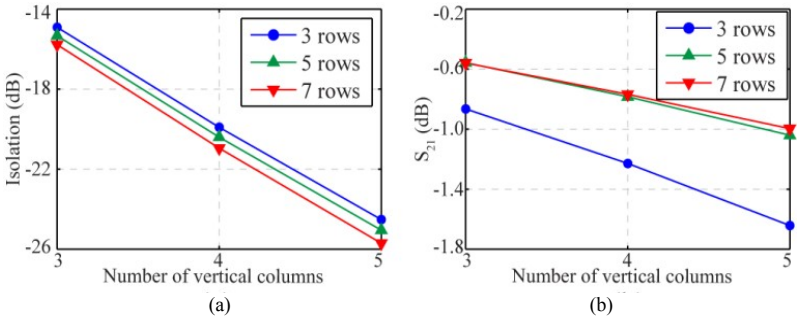

Fig. 2. Design parameter study at 625 GHz to evaluate the influence of the number of vertical columns and horizontal bars: (a) Isolation in the blocking state, and (b) S21 in the non blocking state.

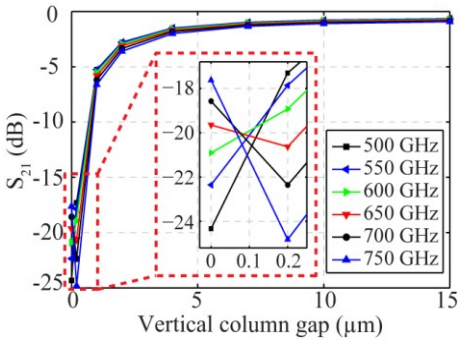

Fig. 3. (Color on line). Design parameter study to evaluate the influence of the vertical column gap on S21, simulated for the lossless case of the nominal design (5 horizontal bars and 4 vertical columns).

The number of vertical columns and horizontal bars has a strong influence on the ability of the MEMS reconfigurable surface to block or unblock the wave propagation. This number is optimized using full-wave simulations to achieve a

low loss transmission through the reconfigurable surface when in the non-blocking state and to achieve a high isolation when in the blocking state. Increasing the number of vertical columns improves the isolation in the blocking state but increases the insertion loss in the non-blocking state. The horizontal bars are perpendicular to the electric field lines in the waveguide and therefore do not impact the performance significantly in non-blocking state. Fig. 2 shows the design optimization simulations carried out at 625 GHz to select the best combination of horizontal bars and vertical columns for the waveguide switch. The design with 5 horizontal bars and 4 vertical columns achieves the best performance where the insertion loss in the non-blocking state is below 0.8 dB and the isolation in the blocking state is below 20 dB. Fig. 3 shows the simulated S_{21} of the nominal design (5 horizontal bars and 4 vertical columns) for different vertical column gaps. There is no significant improvement in the insertion loss for the nonblocking state when the vertical column gap is above 10 μm. A 15 μm gap is selected in the non-blocking state for the designs. Isolation of 20 dB is achieved for a vertical column gap of 200 nm in the blocking state. This gap is used in the simulations to better model the actual contact between the vertical columns. This is needed to compensate for variations in the etch profile and surface roughness of the fabricated designs.

The width of each vertical column is 4 μm with an overlap of 8 μm in the non-blocking state. The rectangular waveguide design has standard WR-1.5 dimensions 380 μm × 190 μm.

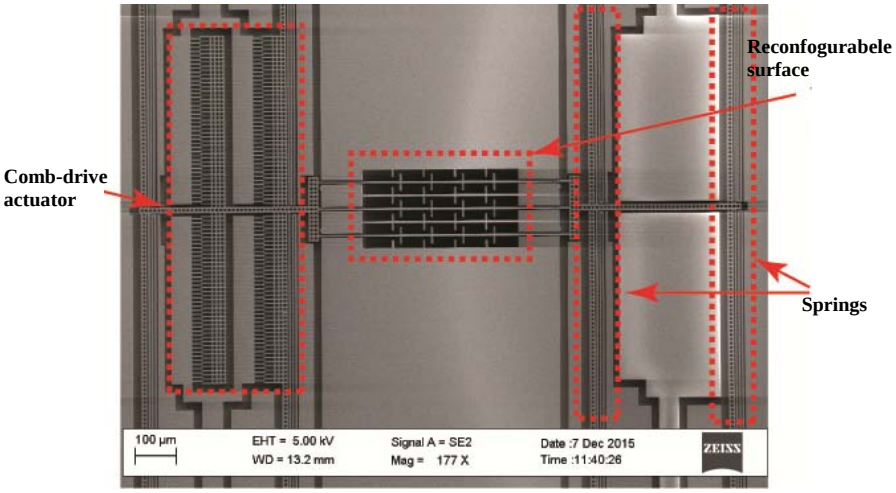

Fig. 4. SEM image of a fabricated prototype device.

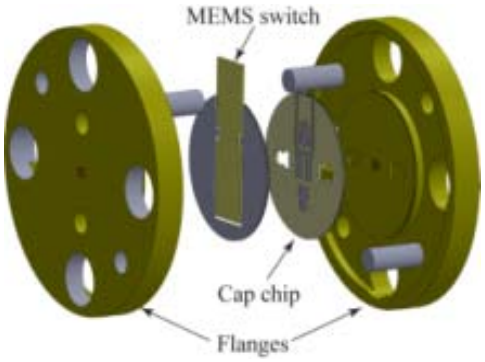

Fig. 5. Exploded 3-D view of mounting/assembly of the MEMS waveguide switch into standard WR-1.5 waveguide.

3. Fabrication and Assembly

The MEMS waveguide switch is fabricated in a two mask SOI RF MEMS micromachining process. The waveguide opening is made by doing the DRIE of the handle wafer (400 μm). This is followed by DRIE of the device layer (30 μm) to make the MEMS reconfigurable surface. The moving structures are free etched by wet etching of the buried oxide layer (3 μm) using hydrofluoric acid which is followed by a critical point drying step. A 900 nm thick gold layer is sputtered on the handle wafer and a 200 nm thick gold layer is sputtered on the device layer. The total chip size including contact pads and bias-line is 3.07 mm × 10.58 mm. Fig. 4 shows an SEM image of a fabricated device.

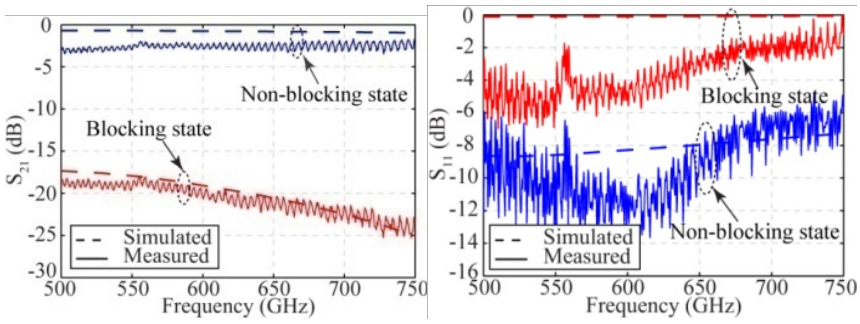

Fig. 6. (Color on line). Measured and simulated normalized S-parameters of the fabricated MEMS waveguide switch (5 horizontal bars and 4 vertical columns) in the two actuation states.

Fig. 5 shows an exploded 3-D schematic drawing, illustrating how the MEMS switch chip is mounted between two waveguide flanges. The MEMS switch chip is aligned to the flanges using omega-shaped alignment structures [8].

4. Measurements

Fig. 6 shows the measured and simulated insertion and return loss of the switch with 5 horizontal bars and 4 vertical columns. The measurements are normalized to a reference measurement done without the MEMS waveguide switch to remove the loss of the measurement fixture. The switch behaves exceptionally broadband over the whole design frequency range of 500-750 GHz with the isolation better than 15 dB in the blocking state. The insertion loss in the nonblocking state is 2 dB higher when compared to the lossless simulation. This is due to the combination of the insufficient gold thickness and surface roughness on the waveguide sidewalls of the MEMS switch. This was confirmed by comparing the insertion losses of two waveguide switches with different gold thicknesses. The measured and simulated return loss shows relatively good agreement except for the higher losses. Fig. 7 shows the measured isolation as the actuation voltage is ramped. The gap between the vertical columns is reduced by increasing the actuation voltage up to 40 V. Increasing the actuation voltage above 40 V no longer influences the isolation implying that the vertical columns make contact at 40 V.

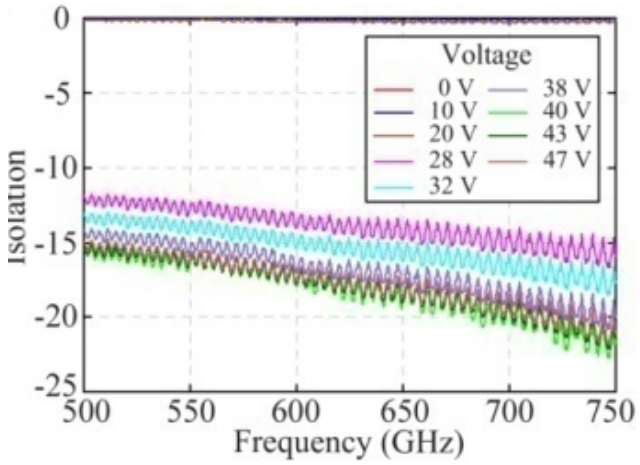

Fig. 7. (Color on line). Measured isolation as a function of applied voltage.

Fig. 8 shows the measured normalized S-parameters of the switch with 5 horizontal bars and 3 vertical columns. Reducing the number of vertical columns from 4 to 3 reduces the isolation in the blocking state from 15 dB (Fig. 6) to 12 dB

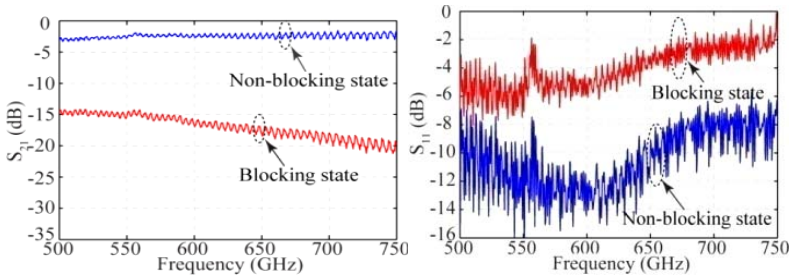

Fig. 8. (Color on line). Measured normalized S-parameters of the fabricated MEMS waveguide switch (5 horizontal bars and 3 vertical columns) in the two actuation states.

at 500 GHz. However, no improvement in the insertion loss in the non-blocking state is observed since the losses are dominated by the waveguide loss in the switch.

5. Conclusion

This paper reported on the design, fabrication and evaluation of the first ever submillimeter-wave MEMS waveguide switch operating in a 40 % bandwidth between 500-750 GHz. The switch has an insertion loss better than 3 dB in the non-blocking state and isolation better than 15 dB in the blocking state. The discrepancy between the measured and simulated insertion loss is attributed to the combination of the insufficient gold thickness and the surface roughness on the waveguide sidewalls.

Acknowledgements. The research described herein is a collaboration effort between the Jet Propulsion Laboratory, California Institute of Technology, Pasadena, California, USA, under contract with National Aeronautics and Space Administration, and KTH Royal Institute of Technology, Stockholm, Sweden.

The contribution by KTH to this work has been funded through the European Research Council Consolidator Grant No. 616846, The Swedish Foundation for Strategic Research Synergy Grant Electronics SE13-007, and through a Nils and Hans Backmark scholarship.

References

[1] K.B. COOPER, and G. CHATTOPADHYAY, *Submillimeter-wave radar: solidstate system design and applications,* IEEE Microw. Mag.,**15**, (7), pp. 51-67, 2014.

[2] M. DANESHMAND and R.R. MANSOUR, *Multiport MEMS-Based Waveguide and Coaxial Switches*, IEEE Trans. Microwave Theory Tech., **53**, (11), pp. 3531-3537, November 2005.

[3] N. VAHABISANI, and M. DANESHMAND, *Monolithic millimeterwave MEMS Waveguide Switch*, IEEE Trans. Microw. Theory Tech., **63**, (2), pp. 340-351, Feb. 2015.

[4] Z. BAGHCHEHSARAEI, and J. OBERHAMMER, *Parameter Analysis of Millimeter-Wave Waveguide Switch Based on a MEMS Reconfigurable Surface*, IEEE Trans. Microw. Theory Tech., **61**, (12), pp. 4396-4406, Dec. 2013.

[5] U. SHAH et. al., *500-600 GHz RF MEMS Based Tunable Stub Integrated in Micromachined Rectangular Waveguide*, 2015 IEEE MTT-S Int. Microwave Symp. Dig., pp. 1-4, May 2015.

[6] U. SHAH et. al., *500-600 GHz Submillimeter-Wave 3.3 bit RF MEMS Phase Shifter Integrated in Micromachined Waveguide*, 2015 IEEE MTT-S Int. Microwave Sy. Dig., pp. 1-4, May 2015.

[7] F. BOUSSAHA, J. KAWAMURA, J. STERN, and C. JUNG-KUBIAK, *2.7 THz Balanced Waveguide HEB Mixer*, IEEE Trans. Microw. Theory Techn., **4**, (5), pp. 545-551, Sep. 2014.

[8] T. RECK, C. JUNG-KUBIAK, J. GILL, and G. CHATTOPADHYAY, *Measurement of silicon micromachined waveguide components at 500-750 GHz*, IEEE Trans. Terahertz Sci. Tech., **4**, (1), pp. 33-38, Jan. 2014.